Supplementary Figures

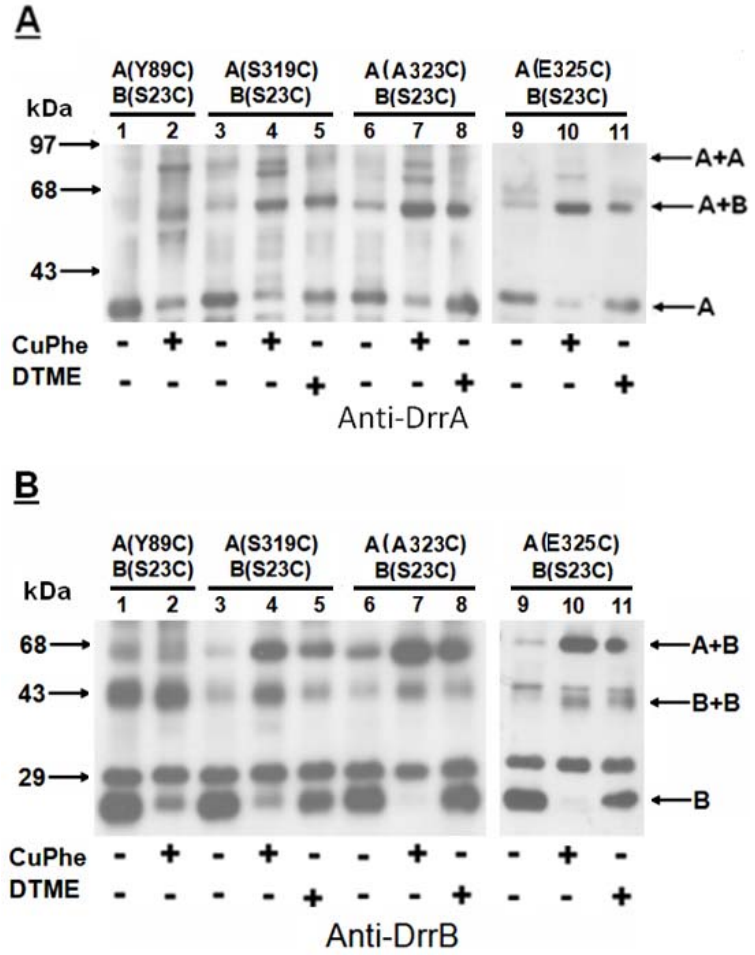

Fig. S1 Disulfide cross-linking between A323C or E325C in DrrA and S23C in DrrB. Two different cross linkers were used: CuPhe and DTME. *Panel* A, anti-DrrA. *Panel* B, anti-DrrB. *Panels* A and B, *lanes* 1, 2: A(Y89C)B(S23C). *Lanes* 3-5: A(S319C)B(S23C). *Lanes* 6-8: A(A323C)B(S23C); *Lanes* 9-11: A(E325C)B(S23C). The plus or minus indicates the presence or absence of the cross linker.

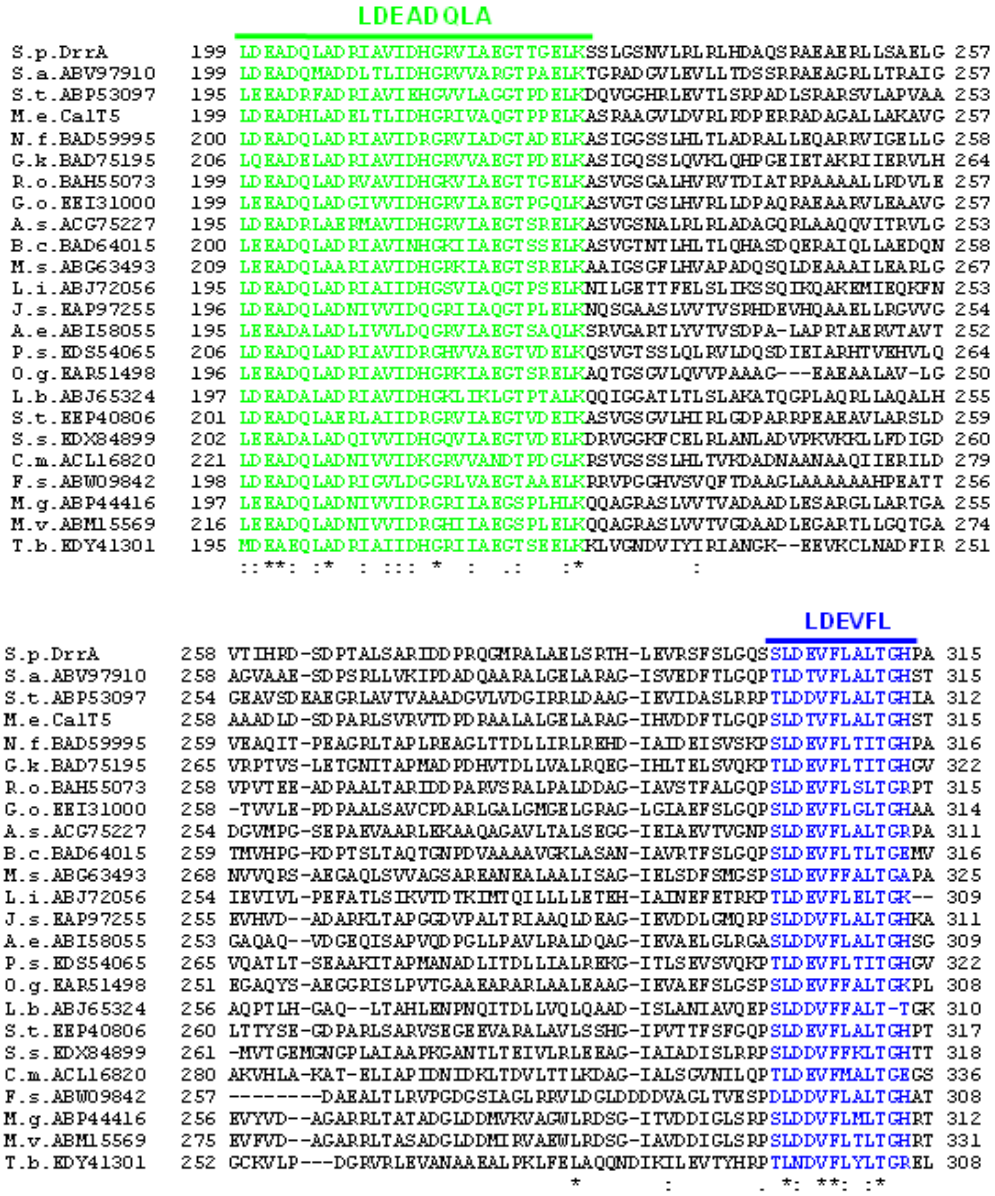

Fig. S2 ClustalW alignment of the C terminal sequence (residues 199-315) of DrrA with the C-terminal sequences of bacterial homologs identified by BLAST search. Sequences in LDEADQLA and LDEVFL motifs are highlighted.

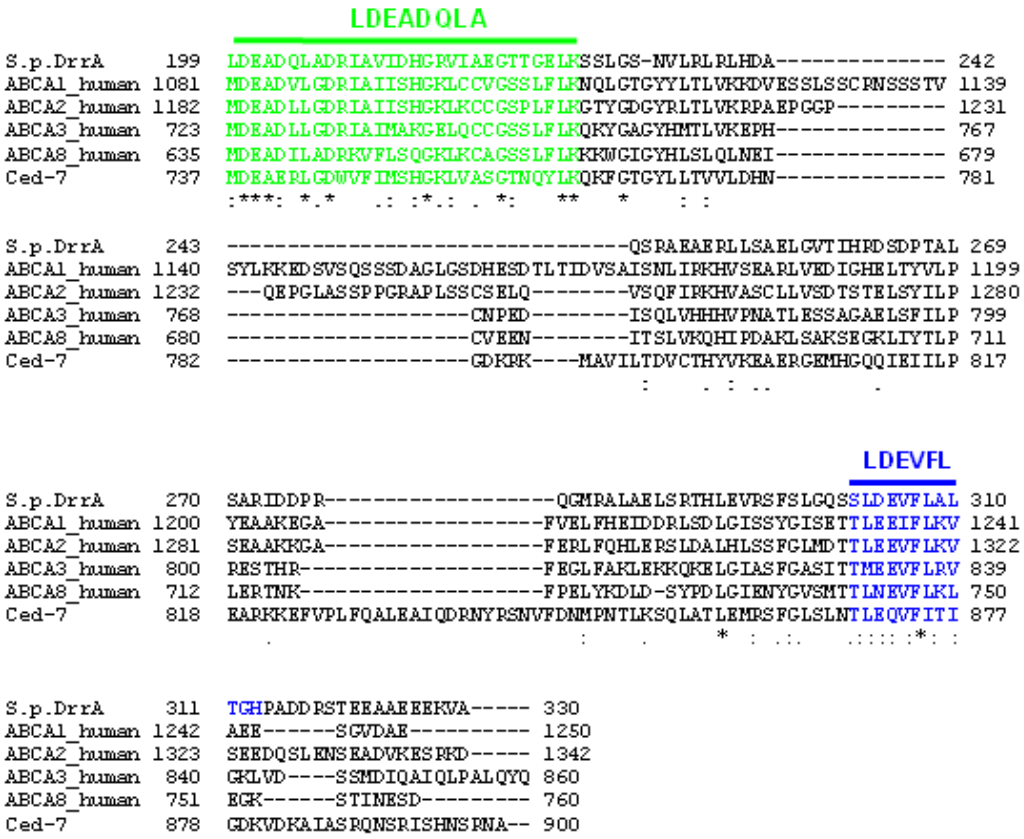

Fig. S3 ClustalW alignment of the last 132 amino acids of DrrA with the C-terminal sequences of NBDI of eukaryotic homologs identified by TC-Blast search. Their homology in LDEADQLA and LDEVFL motifs are highlighted.

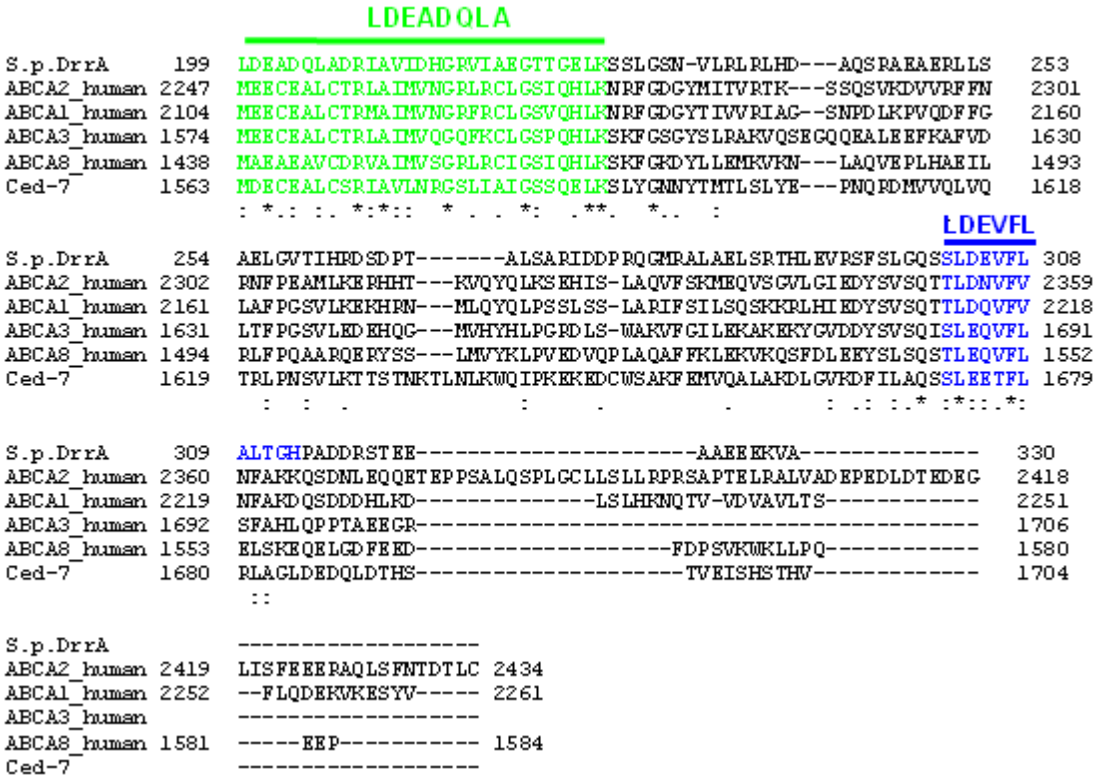

Fig. S4 ClustalW alignment of the last 132 amino acids of DrrA with the C-terminal sequences of NBDII of eukaryotic homologs identified by TC-BLAST search. Their homology in LDEADQLA and LDEVFL motifs are highlighted.

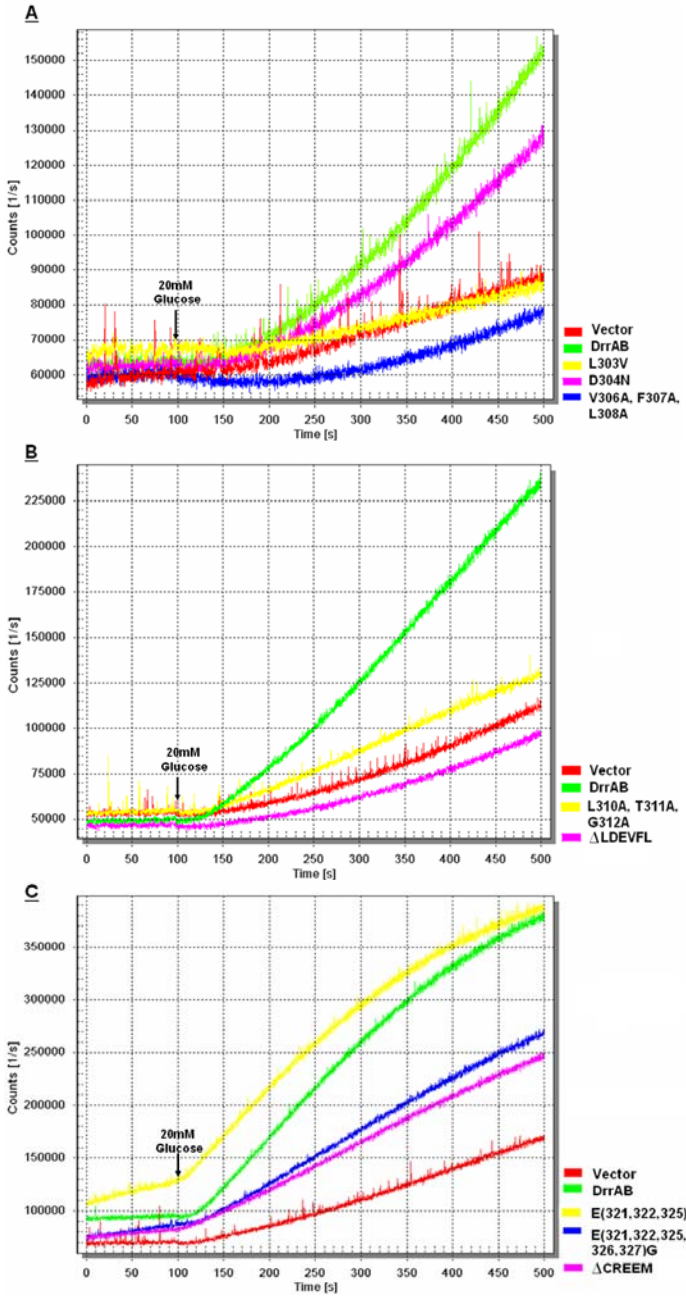
A
Counts [1/s]
Time [s]
20mM Glucose
Vector
DrrAB
L303V
D304N
V306A, F307A, L308A
B
Counts [1/s]
Time [s]
20mM Glucose
Vector
DrrAB
L310A, T311A, G312A
ΔLDEVFL
C
Counts [1/s]
Time [s]
20mM Glucose
Vector
DrrAB
E(321,322,325)G
E(321,322,325, 326,327)G
ΔCREEM

Fig. S5 Effect of LDEVFL or CREEM mutations on doxorubicin efflux. *E.coli* LE392*ΔuncIC* cells containing the indicated plasmids were grown in TEA medium and induced with IPTG at OD=0.6, as described under Methods. Washed cells were de-energized with 5mM DNP and loaded with 10 μM doxorubicin for 11 hours. Loaded cells were washed twice, and doxorubicin fluorecence was measured for 100 seconds. Doxorubicin efflux by the cell suspension was then initiated by providing 20 mM glucose, shown with an arrow. The fluorescence was monitored for additional 400 seconds. The linear region of each curve was used for calculation of the slope of the curve. *Panel* A, effect of L303V, D304N or V306A/F307A/L308A mutation on doxorubicin efflux by DrrAB. The slopes obtained were: vector, 82; wild type DrrAB, 331; DrrA(L303V)DrrB, 63; DrrA(D304N)DrrB, 229; DrrA(V306A/F307A/L308A)DrrB, 84. *Panel* B, effect of L310A/T311A/G312A mutation or ΔLDEVFL in DrrA on doxorubicin efflux by DrrAB. The slopes were: vector, 172; wild type DrrAB, 558; DrrA(L310A/T311A/G312A)DrrB, 220; DrrA(ΔLDEVFL)DrrB, 143. *Panel* C, effect of E(321, 322, 325)G, E(321, 322, 325, 326, 327)G mutation or ΔCREEM on doxorubicin efflux by DrrAB. The slopes were: vector, 233; wild type DrrAB, 930; DrrA(E(321, 322, 325)G)DrrB, 832; DrrA(E(321, 322, 325, 326, 327)G)DrrB, 507; DrrA(ΔCREEM)DrrB, 429.

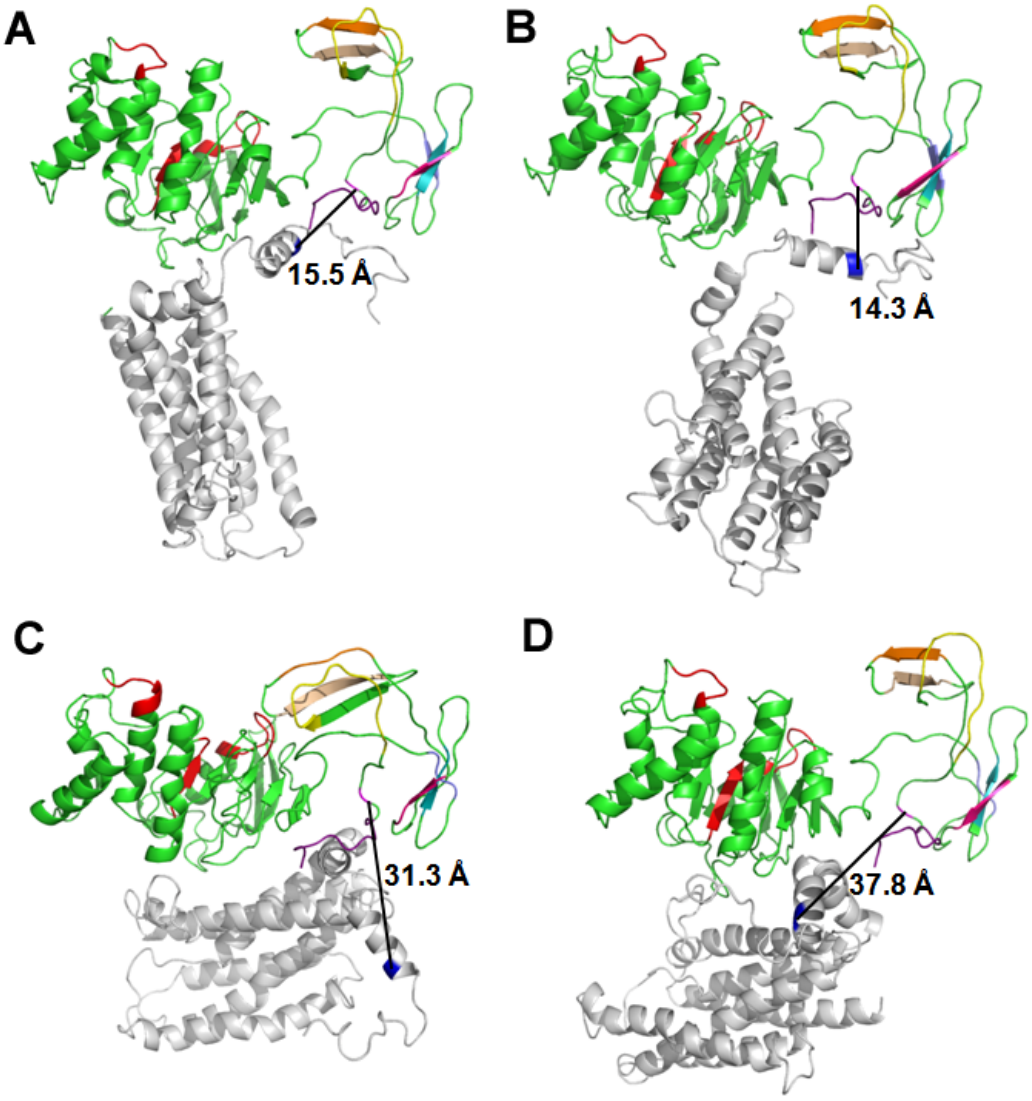

Fig. S6 Docking analysis of the predicted structures of DrrA and DrrB. DrrA protein was modeled using AMMP modeling software and the known structure of MalK as a template. DrrB protein was modeled using the Phyre modeling software (27), as described under Methods. The coordinates obtained for the predicted structures of DrrA and DrrB were then used for docking analysis of DrrA and DrrB by Rosetta Docking server (28). *Panel* A, wild type DrrA and DrrB; *Panel* B, D304N and DrrB; *Panel* C, L303V and DrrB; *Panel* D, X306-308A and DrrB. In all panels, DrrA is shown in green and DrrB is shown in grey. The Walker A, Signature, and Walker B motifs of DrrA are shown in red. The LDEVFL and CREEM motifs in DrrA are shown in yellow and purple, respectively. The β-strands in the C-terminal domain of DrrA are shown in different colors following the same color scheme as seen in Fig. 9. The distances between S319 (shown in magenta) in DrrA and S23 (shown in blue) in DrrB are shown in angstroms.

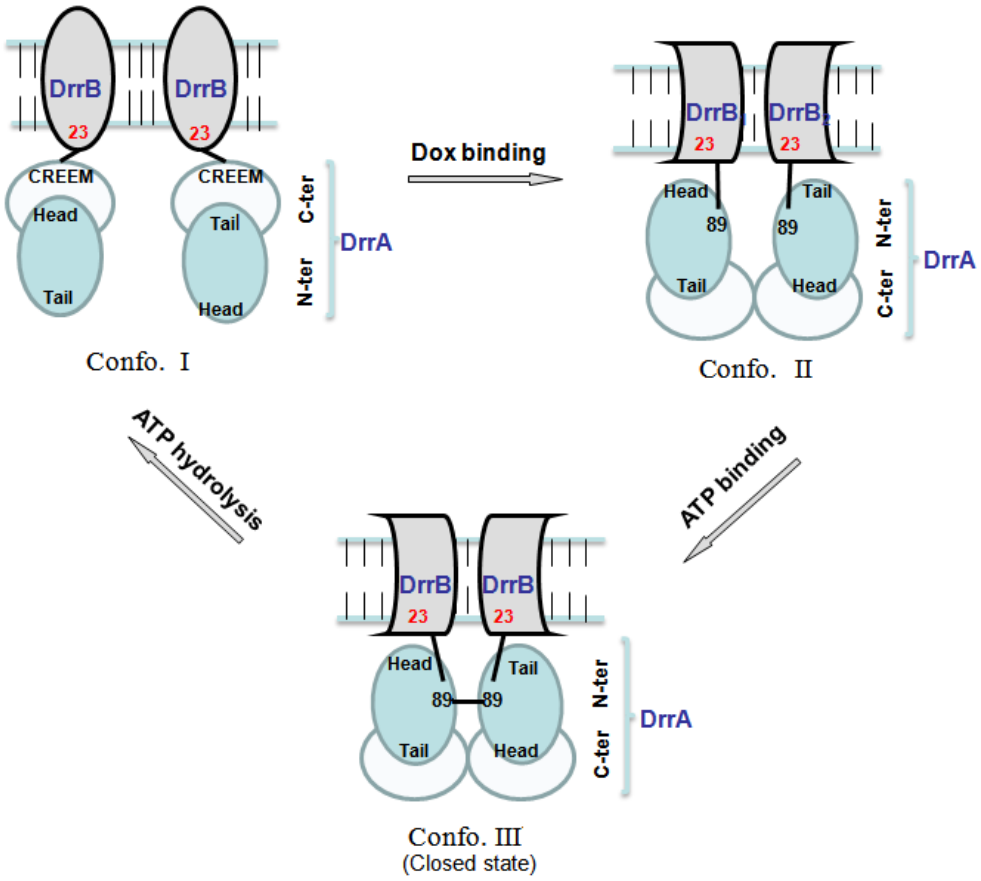

Fig. S7 A model showing various interactions between DrrA-DrrB and DrrA-DrrA during different stages of the catalytic cycle. Both DrrA and DrrB proteins are shown as dimers. DrrA protein contains two domains: an N-terminal nucleotide binding domain (abbreviated as N-ter, filled with blue) in the front, and a C-terminal domain (showing the CREEM motif) (abbreviated as C-ter) in the front. In Conformation I, the two nucleotide binding domains in the N terminus of the DrrA protein are in the open state, while the extreme C terminus of DrrA forms an interface with the N-terminal tail of DrrB. It is proposed that this interaction between the extreme C terminus of DrrA and the N-terminal cytoplasmic tail of DrrB plays a role in assembly and biogenesis of the DrrAB complex. Doxorubicin binding to DrrB produces a conformational change: the extreme C terminus of DrrA disengages from the N-terminal tail of DrrB, which is now involved in communicating conformational changes to the Q-loop region (represented by residue 89) in the N-terminal domain of DrrA (Confo. II). Simultaneously, the extreme C terminus of DrrA undergoes homodimerization. This is followed by the 'closed' state, produced by the head-to-tail dimerization of the NBDs (Confo. III). Hydrolysis of ATP returns the complex to the resting state.